Next-generation bis-locked nucleic acids with stacking linker and 2'-glycylamino-LNA show enhanced DNA invasion into supercoiled duplexes

Geny, Sylvain; Moreno, Pedro M D; Krzywkowski, Tomasz; Gissberg, Olof; Andersen, Nicolai Krog; Isse, Abdirisaq J; El-Madani, Amro; Lou, Chenguang; Pabon, Y Vladimir; Anderson, Brooke A; Zaghloul, Eman M; Zain, Rula; Hrdlicka, Patrick J.; Jørgensen, Per Trolle; Nilsson, Mats; Lundin, Karin E; Pedersen, Erik Bjerregaard; Wengel, Jesper; Smith, C I Edvard

Published in:
Nucleic Acids Research

DOI:
10.1093/nar/gkw021

Publication date:
2016

Published online 8 February 2016

Nucleic Acids Research, 2016, Vol. 44, No. 5 ***2007–2019***
doi: 10.1093/nar/gkw021

Next-generation bis-locked nucleic acids with stacking linker and 2′-glycylamino-LNA show enhanced DNA invasion into supercoiled duplexes

Sylvain Geny[1], Pedro M. D. Moreno[1,2,†], Tomasz Krzywkowski[3,†], Olof Gissberg[1], Nicolai K. Andersen[4], Abdirisaq J. Isse[4], Amro M. El-Madani[4], Chenguang Lou[4], Y. Vladimir Pabon[1], Brooke A. Anderson[5], Eman M. Zaghloul[1], Rula Zain[1,6], Patrick J. Hrdlicka[5], Per T. Jørgensen[4], Mats Nilsson[3], Karin E. Lundin[1], Erik B. Pedersen[4], Jesper Wengel[4] and C. I. Edvard Smith[1,*]

[1]Department of Laboratory Medicine, Karolinska Institutet and Clinical Research Center, Karolinska University Hospital Huddinge, SE-141 86 Stockholm, Sweden, [2]INEB-Instituto de Engenharia Biomedica, Universidade do Porto, Rua do Campo Alegre 823, 4150-180 Porto, Portugal, [3]Science for Life Laboratory, Department of Biochemistry and Biophysics, Stockholm University, Stockholm, SE-171 21, Sweden, [4]Nucleic Acid Center, Department of Physics, Chemistry and Pharmacy, Nucleic Acid Centre, University of Southern Denmark, 5230 Odense, Denmark, [5]Department of Chemistry, University of Idaho, Moscow, ID 83844, USA and [6]Centre for Rare Diseases, Department of Clinical Genetics, Karolinska University Hospital, SE-171 76 Stockholm, Sweden

Received June 29, 2015; Revised January 07, 2016; Accepted January 08, 2016

ABSTRACT

Targeting and invading double-stranded DNA with synthetic oligonucleotides under physiological conditions remain a challenge. Bis-locked nucleic acids (bisLNAs) are clamp-forming oligonucleotides able to invade into supercoiled DNA via combined Hoogsteen and Watson–Crick binding. To improve the bisLNA design, we investigated its mechanism of binding. Our results suggest that bisLNAs bind via Hoogsteen-arm first, followed by Watson–Crick arm invasion, initiated at the tail. Based on this proposed hybridization mechanism, we designed next-generation bisLNAs with a novel linker able to stack to adjacent nucleobases, a new strategy previously not applied for any type of clamp-constructs. Although the Hoogsteen-arm limits the invasion, upon incorporation of the stacking linker, bisLNA invasion is significantly more efficient than for non-clamp, or nucleotide-linker containing LNA-constructs. Further improvements were obtained by substituting LNA with 2′-glycylamino-LNA, contributing a positive charge. For regular bisLNAs a 14-nt tail significantly enhances invasion. However, when two stacking linkers were incorporated, tail-less bisLNAs were able to efficiently invade. Finally, successful targeting of plasmids inside bacteria clearly demonstrates that strand invasion can take place in a biologically relevant context.

INTRODUCTION

Efficient and sequence-specific targeting of double-stranded DNA (dsDNA) by synthetic ligands is a major objective for treatments based on *in vivo* chromosomal targeting (1), but also for certain aspects of biotechnology, including the generation of highly-defined nanostructures (2). Currently, most strategies targeting dsDNA are dependent on engineered proteins, triplex forming oligonucleotides (TFOs) or minor groove binders (3). Engineered proteins, such as zinc-finger nucleases, bind only certain nucleotide triplets, whereas transcription activator-like effector nucleases (TALENs) are more modular, but larger in size (4), and TFOs do not target outside polypurine/polypyrimidine stretches (5). CRISPR-Cas9 can be directed to essentially any DNA sequence (6,7) and relies on the ability of the very large, exogenous Cas9 protein to preopen the double helix. Double-helix invasion is a highly attractive mechanism for targeting dsDNA due to the simplicity of design, which is based on Watson–Crick pairing rule (8,9). However, dsDNA remains difficult to access due to the stabilizing interactions in the double helix, i.e. base pairing and stacking (10–12).

*To whom correspondence should be addressed. Tel: +46 8 58583651; Fax: +46 8 58583650; Email: edvard.smith@ki.se
†These authors contributed equally to the work as second authors.

Significant efforts have been devoted to develop synthetic oligonucleotides (ONs) with altered backbone to invade into intact dsDNA. Peptide nucleic acid (PNA) was the first synthetic ON capable of invasion, but this activity is essentially confined to non-physiological, 'low salt' conditions (13,14), thus limiting the utility of this strategy *in vivo* (14–16). Despite this drawback, bisPNA, clamp-constructs (17) found numerous applications due to their ability to combine both Watson–Crick (WC) and Hoogsteen (HG) binding, thereby considerably enhancing hybridization (18,19). As an alternative synthetic chemistry, locked nucleic acid (LNA), another class of nucleotide analogues, is reported to invade into supercoiled DNA (20–22). LNA-ONs are characterized by a conformationally restricted sugar with a methylene linkage between the 2′ oxygen and the 4′ carbon (23,24).

Recently developed, the bis-locked nucleic acids (bisLNA) are clamp-ONs that combine the positive LNA contribution in a triplex-forming arm (TFO-arm) connected via a linker to an invading arm (WC-arm). The bisLNAs recognize polypurine/polypyrimidine sequences with high specificity under physiological conditions. Although non-clamp LNA-ONs are able to invade, bisLNAs form extremely stable triplexes that withstand DNA relaxation, thus demonstrating more potent binding than their respective WC-arms alone (25). In addition, LNA-phosphoramidite chemistry has the advantage of being readily compatible with a range of chemical modifications.

Among other modifications available, twisted intercalating nucleic acid (TINA) is a flexible intercalator inserted as a bulge to considerably stabilize the triple helix (26). Modified linkers with aromatic moieties confer the ability of stacking to adjacent nucleobases to form highly stable and sequence-specific triplexes (27,28). Recently, LNA analogues have been developed to enhance WC- and HG-interactions, in particular 2′-amino-LNA (29–31) and C5-functionalized LNA pyrimidines (32). However, predictive models to guide the design of invading ONs are lacking. Due to that, an experimental trial-and-error process has been the only possible approach to develop more efficient invading ONs. Therefore, understanding the molecular mechanism of invasion is critically important to design efficient bisLNAs.

In this study, we investigated the binding mechanism for bisLNAs. We synthesized a series of bisLNAs modified with TINAs, novel stacking linkers and positively charged LNA analogues to assess their potential for DNA invasion under physiological conditions. Additionally, to evaluate their sequence-specificity, we developed an S1 nuclease footprinting method based on capillary electrophoresis separation. Finally, we demonstrated that bisLNAs invade target plasmids when present inside *Escherichia coli* bacteria.

MATERIALS AND METHODS

Oligonucleotides

Oligonucleotides were synthesized by solid phase phosphoramidite chemistry on an automated DNA synthesizer in 1.0 micromole synthesis scale with 20 min coupling time for monomers **M2**, **M3** and **N2**. Purification to at least 80% purity of all modified ONs was performed by RP-HPLC or IE-HPLC, and the composition of all synthesized ONs was verified by MALDI-MS analysis recorded using 3-hydroxypicolinic acid as a matrix. The syntheses of **M2**, **M3** and **N2** phosphoramidites are reported in the Supplementary Information. The ONs used in this work are presented in Table 1.

Plasmid hybridizations

Plasmids (1 μg, 100 ng/μl) were hybridized with LNA-ONs, at different final concentrations (0.05, 0.15, 0.45, 1.35, 4.05 and 12 μM, corresponding to an LNA-ON/plasmid ratio of, respectively, 2.5, 7.6, 22.7, 68.2, 205, 614). Hybridizations were carried out at 37°C in an oven incubator for 16 h or 72 h. The hybridization was performed in a buffer containing 50 mM tris-acetate (pH 7.3–7.4), 120 mM KCl, 5 mM NaCl and 1 mM $Mg(OAc)_2$, corresponding to intranuclear conditions. The plasmids used in this work are presented in Table 2.

S1 nuclease assay

Plasmid (250 ng), pre-hybridized with bisLNA, was incubated with 24 units of S1 enzyme (Promega) in a total volume of 11 μl at 4°C for 6 min. The reaction was stopped by the addition of EDTA (500 mM, 3 μl). A volume of 1.5 μl of the final solution was loaded and run in a 0.9% agarose gel (Tris-Boric-Acid-EDTA buffer (TBE 0.5x) containing SYBRGold (Life Technologies) and analyzed on a Versadoc using the QuantityOne software. Quantification of the invasion was determined after electrophoresis by calculating the ratio of nicked plasmid to the total plasmid amount in a sample relatively to the same ratio in the mock hybridized sample.

Restriction digestions and agarose electrophoretic mobility shift assay (A-EMSA)

Plasmid (500 ng), pre-hybridized with bisLNA (12 μM, 16 h) was digested with XhoI and SmaI (FastDigest, Fermentas). The subsequent gel electrophoresis was performed in a freshly prepared 2% agarose TBE 1X gel containing 2 mM $MgCl_2$ at 4°C (120 V, 1 h 45 min). After electrophoresis, the gel was stained with SYBR Gold (Life Technologies) and analyzed in the VersaDoc system (BioRad) using the QuantityOne software (Biorad).

S1 nuclease footprinting via capillary electrophoresis

Plasmid pEGFP-BSf (500 ng) pre-hybridized with bisLNA (4 μM, 72 h) was digested with S1 nuclease following protocol described above. After digestion, the samples were purified using Spin columns (Qiagen PCR purification kit) according to the manufacturers protocol. The plasmids were subsequently linearized using NdeI and SacI (Fermentas). Primer extension was carried out under the following conditions: [2 mM $MgCl_2$, 3 U Taq polymerase (Fermentas), 2.5 nM primer, 2 mM of each dNTP. Ten minutes at 94°C, 29 cycles of 1 min at 94°C, 2 min at 45°C, 3 min at 72°C and finally 10 min at 72°C. Primer sequence: 5′ 6FAM-AAA TGG GCG GTA GGC GT 3′ (Cybergene)]. Plasmid was sequenced using Thermo Sequenase Primer Dye Manual Cycle Sequencing kit (Affymetrix). For each sample, 5 μl of the

Table 1. List of the oligonucleotides used in this work

Oligonucleotides		Sequence 5′-3′
bis-m44, -N2,-M2, -M3	R = tctct, R = N2,M2,M3	Cy3-CcTtTtCtTtTtTcT-R-tCtTtTtTcTtTtCcCccAcgCccTctGc
TFO-m44 / WC-m44		Cy3-CcTtTtCtTtTtTcT / Cy5-tCtTtTtTcTtTtCcCccAcgCccTctGc
bis-TFO1		Cy3-ccttttCtTtTtTcT-tctct-tCtTtTtTcTtTtCcCccAcgCccTctGc
bis-TFO2		Cy3-CcTtTtCttttttct-tctct-tCtTtTtTcTtTtCcCccAcgCccTctGc
bis-TINA1		Cy3-CcTtTtCtTtTtTcPT-tctct-tCtTtTtTcTtTtCcCccAcgCccTctGc
bis-TINA2		Cy3-CcTtTtCtTtTtTcT-tctct-tPCtTtTtTcTtTtCcCccAcgCccTctGc
bis-TINA3		Cy3-CcTtTtCtTtTtTcT-tctct-tCtTtTtTPcTtTtCcCccAcgCccTctGc
bis-TINA4		Cy3-CcTtTtCtTtTtTcT-tctct-tCtTtTtTcTtTtCcPCccAcgCccTctGc
bis-TFOm-M3		CtTtCtTtTtCtTcT-M3-tCtTtTtTcTtTtCcCccAcgCccTctGc
WC-m44-M3		M3-tCtTtTtTcTtTtCcCccAcgCccTctGc
bis-m37, -M3	R = tctct,M3	Cy3-CcTcCcTcCcT-R-TcCcTcCcTcCgTtCtTtTtCcCgCc
bis-ERE		GaCcXaCaggXcaCaAtGaCcXtCcXtXcCtC-M3-CtCcXtXcCtXcC
bis-hTFF		CcCtXcCcXtCcT-M3-TcCtXcCcXtXcXtXtGcaAggXcaCggXggCc
bis-m30		Cy3-cCtTtTcTtTtTtCt-tctct-TcTtTtTtCtTtTcC
bis-m30-gly		Cy3-cCtXtTcXtXtXtCt-tctct-TcXtXtTtCtXtXcC
bis-m30-pip		Cy3-cCtZtTcZtZtZtCt-tctct-TcZtZtTtCtZtZcC
bis-m44-prop		Cy3-CcWtWtCtWtTtWcT-tctct-tCtWtTtWcTtWtCcCccAcgCccWctGc
bis-m44-gly		Cy3-YcXtXtYtXtXtXcX-tctct-tYtXtXtXcXtXtYcYccAcgCccTctGc
bis-m44-gly-M3		Cy3-YcTtXtCtXtTtXcT-M3-tCtXtTtTcXtTtCcYccAcgCccXctGc
bis-2M3		Cy3-M3-CcTtTtCtTtTtTcT-M3-tCtTtTtTcTtTtCc
bis-2M3gly		Cy3-M3-cCtXtTcXtXtXtCt-M3-TcXtXtTtCtXtXcC
bis-tail-M3		Cy3-CcTtTtCtTtTtTcT-M3-tCtTtTtTcTtTtCcCccACgCCcTCtGC

LNA nucleotides are in capital letters; DNA nucleotides are in small letters; linker sequence is underlined; P: twisted intercalating nucleic acid (TINA), W: 5′-propargylamino-LNA-U, X: 2′-glycylamino-LNA-T, Y: 2′-glycylamino-LNA-5-MeC, Z: 2′-(3-piperazinopropanoyl)amino-LNA-T; N2, M2, M3: modified linkers.

Table 2. Plasmids used in this study and respective target sequences

Plasmids	Sequences
pDel-1 P1/ pEGFP-BSf	5′-AAAGCAGAGGGCGTGGG**GGAAAAGAAAAAAGA**TCCT-3′ 3′-TTTCGTCTCCCGCACCCCCTTTTCTTTTTTCTAGGA-5′
pDel-1 P2	5′-GGCTTGGCGGGAAAAAGAAC**GGAGGGAGGGA**TCGCGC-3′ 3′-CCGAACCGCCCTTTTTCTTGCCTCCCTCCCTAGCGCG-5′
ERE	5′-CTAGT**GAGGAAAGGAAGG**TCACTGTGACCTGTAGGTCACACT-3′ 3′-GATCACTCCTTTCCTTCCAGTGACACTGGACATCCAGTGTGA-5′
hTFF	5′-GGGTGGCCACCGTGACCTTGCAGG**GGGAAGGGAAGGA**GCTCAT-3′ 3′-CCCACCGGTGGCACTGGAACGTCCCCCTTCCCTTCCTCGAGTA-5′

Underlined bases indicate the binding site of bisLNAs via Watson–Crick interaction. Bold letter indicate the binding sites via Hoogsteen interaction.

PCR reaction, 4.75 μl of HiDi (Life Technologies) and 0.25 μl of GeneScan 600-LIZ (Life Technologies) were analyzed using ABI 3730 DNA Analyzer (injection voltage 3 kV, 30 s). The electropherograms were analyzed with GeneMapper 5 (Life Technologies) and horizontally aligned in the sample plot window through the use of the size standard. The reactions from the Thermo Sequenase kit were superimposed and aligned to the digestion samples to read the sequence.

Rolling circle amplification (RCA)

The *E. coli* DH5α bacterial strain, transformed with target plasmid pUC19–2BS or control plasmid pUC19 was grown overnight in LB medium containing ampicillin (100 ng/ml). After centrifugation (3000 g for 20 min), the bacterial pellet was washed twice with phosphate buffered saline (PBS) and then resuspended in 200 μl ice-cold methanol/ acetic acid (3:1) for 20 min. Bacteria were placed on microscope slides to dry and then stored at 4°C. In order to limit the reaction volume, slides containing attached cells were covered with 8 mm diameter Secure Seal chambers (Invitrogen) ∼50 μl total volume. Hybridizations with bisLNA were performed at 37°C for 72 h in secure seal chambers with 2 μM bisLNA in the intranuclear buffer. Reaction chambers were then washed in 1xBuffer-B (2x SSC, 0.05% Tween-20) for 5 min at 25°C followed by two rounds of washes in 1X Buffer-A (0.1 M Tris-HCl pH 7.5, 0.15 M NaCl, 0.05% Tween-20) for 5 min at 25°C. Padlock probe ligation on the displaced DNA strand was performed in 1xT4 ligase buffer (DNA Gdansk) with 2 μM padlock probe, 1 mM ATP (DNA Gdansk), 0.25 M NaCl, 0.1 U/μl T4 Ligase (DNA Gdansk) for 2 h at 25°C. Slides were washed twice in 1xBuffer-B for 5 min at 25°C and ligated padlock probes were amplified by RCA. The reactions were performed in 1xPhi29 Polymerase buffer (Fermentas) with 0.2 μg/μl BSA (New England Biolabs), 0.20 mM dNTPs (Fermentas), 2 μM primer and 0.2 U/μl Phi29 DNA Polymerase (Monserate Biotechnology Group) overnight at 25°C. Finally, rolling circle products (RCPs) were counter stained by hybridizing 0.1 μM detection ONs with 1 mM Hoechst 33342 (Sigma), 20% formamide and 2x SSC in DEPC-PBS for 20 min at 25°C. After two washes with 1xBuffer-A, secure seals chambers were removed, slides were dehydrated with 99.5% ethanol (3 min), air dried and mounted with SlowFade mounting medium (Life Technologies). Bacterial slides were evaluated with an AxioplanII epifluorescence microscope (Zeiss)

equipped with Orca Flash 4.0 v2 camera (Hamamatsu) with a total 400x magnification using ZEN software.

Molecular modeling

Molecular modeling was performed with Macro Model v9.1 from Schrödinger. All calculations were conducted with the AMBER* force field and the GB/SA water model. The dynamic simulations were performed with stochastic dynamics, a SHAKE algorithm to constrain bonds to hydrogen, time steps of 1.5 fs and simulation temperature of 300 K. Simulation for 0.5 ns with an equilibration time of 150 ps generated 250 structures, which all were minimized using the PRCG method with convergence threshold of 0.05 kJ/mol.

RESULTS

Triplex formation affects invasion into the underlying duplex

To better understand the binding properties of bisLNA, we investigated the effect of triplex formation on DNA strand-invasion (DSI). To quantify DSI, we used a fine-tuned S1 nuclease assay, based on the ability of the S1 nuclease to specifically cut single-stranded DNA. Invasion into the plasmid results in a local displacement of one strand, which can be quantified in terms of plasmid nicking after S1 nuclease treatment. To assess precisely the role of the TFO-arm, we compared the DSI between the WC-arm alone (WC-m44) and the unlinked arms (TFO-m44/WC-m44) (Figure 1A). Interestingly, WC-m44 exhibited higher DSI alone than when co-incubated with TFO-m44 (31% DSI at 12 μM) (Figure 1B), despite that no interaction is predicted between the two arms. Likewise, similar results were achieved with the unlinked arms TFO-A1/WC-A1 when targeting another site A1, which confirms that this effect is sequence independent (Supplementary Figure S2C). We hypothesized that the TFO-arm, once hybridization is established, forms a triplex structure that sterically reduces the accessibility for the WC-arm into the underlying duplex. It is noteworthy that both bis-m44 and bisA1 showed similar DSI as their respective WC-arms. Although the TFO-arm is expected to improve the target recognition, it may also reduce DSI. To verify this assumption, we designed bisLNAs containing less LNA in the TFO-arm either in the 5′- or 3′-extremity (bis-TFO1, bis-TFO2) (Figure 1C). For both constructs, melting assays confirmed the TFO binding ($T_m = 52°C$) despite the reduced number of LNA nucleotides (Supplementary Figure S2B). Surprisingly, both bis-TFO1 and bis-TFO2 were less efficient (8% and 22% DSI at 12 μM) than their respective WC-m44 (Figure 1D). This suggests that the binding of the TFO-arm reduces DSI under certain conditions in bisLNAs, as observed for the unlinked arms, and therefore requires an optimized design.

TINA has different effects depending on the position in the bisLNA

To increase the triplex stability, we designed bisLNAs with the triplex intercalator known as TINA (Figure 2A and B) (26,33). To ensure that TINA-containing bisLNAs tether correctly to the plasmid, we assayed binding using S1 nuclease (Figure 2C) and EMSA (Figure 2D) (34). The S1 nuclease measures the DSI relative to the WC-arm whereas the EMSA estimates the overall binding stability of the bisLNAs. In EMSA, the linearization of the plasmid removes the negative supercoiling, thereby providing a 'kick out' effect that will dissociate the previously bound non-clamp LNA-ON (35). According to our previous study, bisLNAs withstand linearization due to their combined HG- and WC- base pairing (25).

We found that different positioning of the TINA significantly changes the binding properties of the bisLNAs. The bis-TINA1 (TINA in the TFO-arm) showed moderate DSI (29% at 12 μM), but essentially complete binding after linearization, as observed by the fully shifted band in EMSA. This strong affinity arises presumably from the TINA-induced triplex binding despite an incomplete invasion, forming a triplex with a dangling tail. Similarly, TFO-m44-TINA and bis-TINA5 exhibited full binding after linearization without WC-binding, as a consequence of the TINA being placed in the TFO-arm (Supplementary Figure S3). When the TINA was inserted in the WC-arm, bis-TINA2 and bis-TINA3 showed moderate DSI (39% and 57% at 12 μM) in agreement with their respective shifts in EMSA (Figure 2C and D). This confirms that these bisLNAs form stable triplexes upon binding via both HG- and WC-interactions. Interestingly, bis-TINA4 (TINA in the WC-arm at the tail/clamp junction) showed the highest DSI (71%). However, the absence of a retarded band in EMSA indicates that the final complex binds in an experimentally unstable and unpredictable way. Altogether, TINAs were found to be more suitable for the purpose of TFO stabilization than for DSI.

Stacking of the linker M3 to adjacent nucleobases enhances bisLNA invasion

Based on our results, it appears that the linker is crucial for promoting DNA invasion into the duplex. With this in mind, we designed asymmetric bisLNAs with shorter TFO-arm and extended WC-arm in the vicinity of the linker to reduce the distance to connect the arms. To the best of our knowledge, this design was never previously tested in a clamp-ON and could make it possible to use shorter nucleotidic linkers (2–3 nt) (Supplementary Figure S4A–C). However, these asymmetric bisLNAs were not more efficient than the original bis-m44 (Supplementary Figure S4D).

Next, we examined the effect of linkers capable of stacking to adjacent nucleobases. These new linkers combine a stiff conjugated aromatic moiety with conformational flexibility as the triple bonds allow better stacking to the underlying bases in the formed triplex. To assess how this extra stabilization affects the DSI, we substituted the pentanucleotide linker in bis-m44 by three linkers, named N2, M2 or M3 (Figure 3A). As a result, bis-m44-N2 and bis-m44-M2 showed respectively decreased DSI (16% at 12 μM) or similar DSI (49% at 12 μM), as compared to bis-m44 (Figure 3B, upper panel). Interestingly, bis-m44-M3 exhibited considerably higher DSI (83% at 12 μM) and a completely retarded band in EMSA (Figure 3C). Thus, the bis-m44-M3 demonstrates high stability after linearization. Consis-

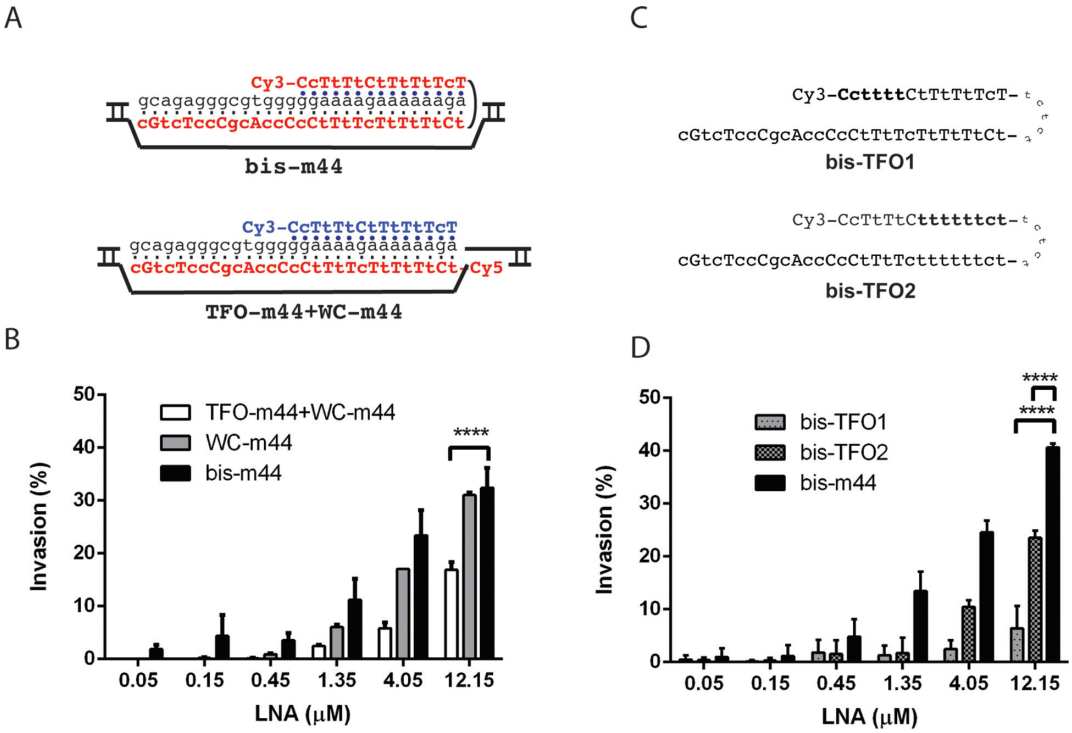

Figure 1. The TFO-arm effect on the dsDNA invasion (**A**) A schematic illustration of a triplex formed by bis-m44 or unlinked arms (WC-m44+TFO-m44) with their target sequence. Filled and open circles indicate respectively Watson-Crick and Hoogsteen base pairs. (**B**) Invasion of bis-m44, its WC-arm (WC-m44), and unlinked arms (WC-m44+TFO-m44). (**C**) Schematic illustration of bis-TFO1 and bis-TFO2 with reduced LNA content in the TFO-arms. Modified triplex forming oligonucleotides (TFO) region is indicated in bold letter. (**D**) Invasion of bis-TFO1 with LNAs in the 3′-end and bis-TFO2 with LNAs in the 5'-end of the TFO-arm. For (A,C), LNA bases are in capital letters; DNA bases are in small letters. For (B,D), plasmid p-Del1 was incubated for 16 h at 37°C at intranuclear pH and salt conditions with different LNA-ON concentrations. Quantification of invasion was performed using the S1 nuclease assay.

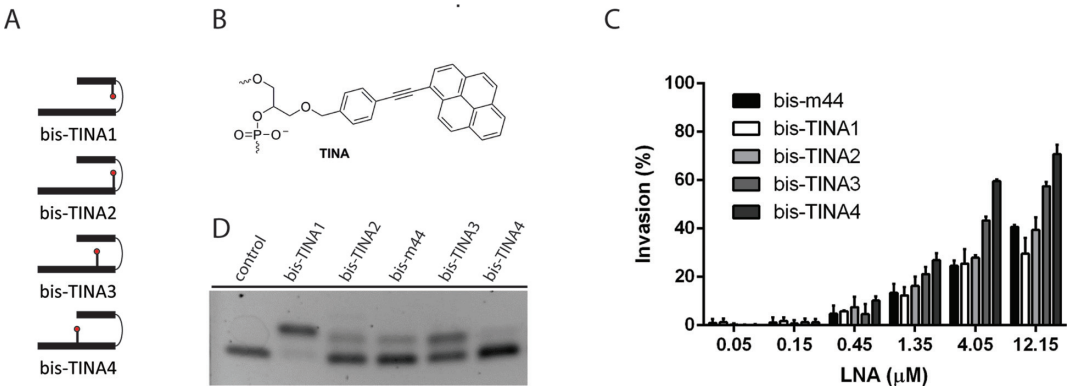

Figure 2. Effect of twisted intercalating nucleic acids (TINA) in bisLNAs. (**A**) Schematic illustration of the positioning of TINA within the bisLNAs. (**B**) Chemical structure of TINA (**C**) Quantification of invasion using S1 nuclease assay. Plasmid p-Del1 and bisLNAs were incubated 16 h at 37°C at intranuclear pH and salt conditions. (**D**) Agarose electrophoretic mobility shift assay (EMSA) showing the relative binding strength of different TINA-containing bisLNAs after digestion-induced linearization of plasmid p-Del1. Plasmid p-Del1 was incubated 16 h at 37°C with 12.15 μM bisLNA at intranuclear pH and salt conditions.

tent with this, the melting temperatures of M3-containing bisLNAs were too high to be measured accurately (data not shown). Nevertheless, the benefit of the linker M3 was significantly reduced when the tail was shortened from 14 to 7 nt (Supplementary Figure S5A–B).

As a control, we synthesized a non-clamp WC-m44-M3 with an M3 moiety attached at the 3′ extremity that invaded significantly less well as compared to bis-m44-M3 (34% versus 80% at 12 μM) (Figure 3B, lower panel) due to the absence of the TFO-arm. To further investigate the importance of the triplex region, we synthesized bis-TFOm-M3 containing a scrambled TFO-arm. Interestingly, bis-TFOm-M3 failed to invade efficiently (19% at 12 μM) although the WC-arm was fully complementary to its target. Apparently, the dangling TFO-arm has a detrimental effect that makes bis-TFOm-M3 even less efficient than WC-

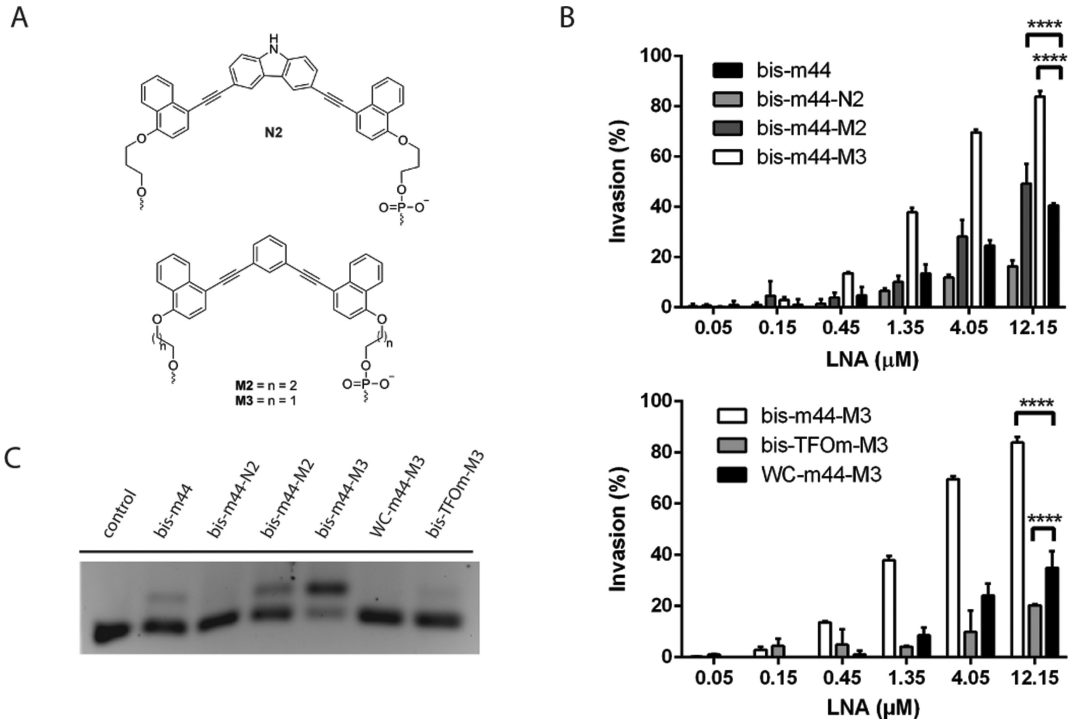

Figure 3. The linkers stacking to the adjacent nucleobases. (**A**) Chemical structure of linkers N2, M2 and M3. (**B**) Quantification of invasion using S1 nuclease assay. Comparison between bis-m44 and bis-m44-N2,-M2,-M3 (upper panel). Comparison between bis-m44-M3, its respective M3-containing WC-arm (WC-m44-M3), and the same WC-arm connected by the M3 linker to a mutated TFO (bis-TFOm-M3) (lower panel). Plasmid p-Del1 and bisLNAs were incubated for 16 h at 37°C with 12.15 μM LNA-ON at intranuclear pH and salt conditions (**C**) Agarose EMSA showing the relative binding strength of bisLNAs containing a stacking linker after digestion-induced linearization of plasmid pDel-1.

m44-M3 (34% at 12 μM). In EMSA, both bis-TFOm-M3 and WC-m44-M3 did not display binding after linearization despite the presence of linker M3. It is remarkable that the linker M3 selectively stabilizes only a properly formed bisLNA triplex.

Our structural model (Figure 4, top view) indicates a π–π-stacking interaction between the terminal nucleobases and the linkers M2/M3. The model (Figure 4, side view) also suggests an increased rigidity for linker M3 in relation to M2, which correlates with better stacking and DSI for the linker M3. This demonstrates that careful linker design is crucial to promote invasion, since both the M2 and M3 have nearly similar structures but result in significantly different DSI.

2′-glycylamino-LNA and linker M3 enhance bisLNA invasion at low concentration

Triplexes are generally less stable than the corresponding duplexes as a result of the assembly of three negatively charged strands (36). To promote triplex formation, we incorporated positively charged LNA analogues, such as 2′-(3-piperazinopropanoyl)amino-LNA (pipLNA) (37,38), 2′-glycylamino-LNA (glyLNA) (30) or 5′-propargylamino-LNA-U (propLNA) (39)(Figure 5A). First, we compared these modifications in clamp-type bisLNAs (Figure 5B) because, as previously reported, bisLNA clamps exhibit low invasion (<5% at 12 μM, 72 h) (25). We observed a positive contribution from glyLNA in bis-m30-gly, although DSI is still limited (20%). In contrast, we did not detect improvement in DSI with bis-m30-pip (5%, 12 μM), despite the additional positive charges in pipLNAs.

We next incorporated modifications in bisLNAs tail-clamp (Figure 5C). Despite the presence of propLNAs, bis-m44-prop showed no significant difference compared to the unmodified bis-m44. As expected, the bis-m44-gly showed further enhancement in DSI, efficient already at 150 nM, although it reaches only 40% DSI at 12 μM after 16 h and 60% after 72 h incubation. We assumed that the incomplete DSI is due to the high number of glyLNAs. This led to the synthesis of bis-m44-gly-M3 (fewer glyLNA and a linker M3), resulting in already 40% DSI at 0.45 μM and 80% at 12 μM. In comparison, we tested bis-tail-M3 (a linker M3 and high LNA content in the tail), which showed similar DSI. As such, glyLNA enables the reduction of the total number of LNA nucleotides while achieving the same invasion efficiency.

To reduce the length of bisLNAs, we designed bisLNA clamps with two stacking moieties, one as a linker connecting the arms and one to the termini of the TFO (Figure 5D). Remarkably, the bis-2M3 showed DSI (18% at 12 μM), despite the absence of a tail. Furthermore, bis-2M3gly including glyLNA resulted in higher DSI (51% at 12 μM). It is worth noting that after 72 h incubation, both bis-2M3 and bis-2M3gly reached higher DSI (36% and 60%) (Supplementary Figure S5C). This indicates that the stacking of the M3 moieties at the triplex extremities favors greatly DSI. Importantly, this strategy is not applicable to bisLNAs tail-clamp because the tail is a steric hindrance at the triplex-

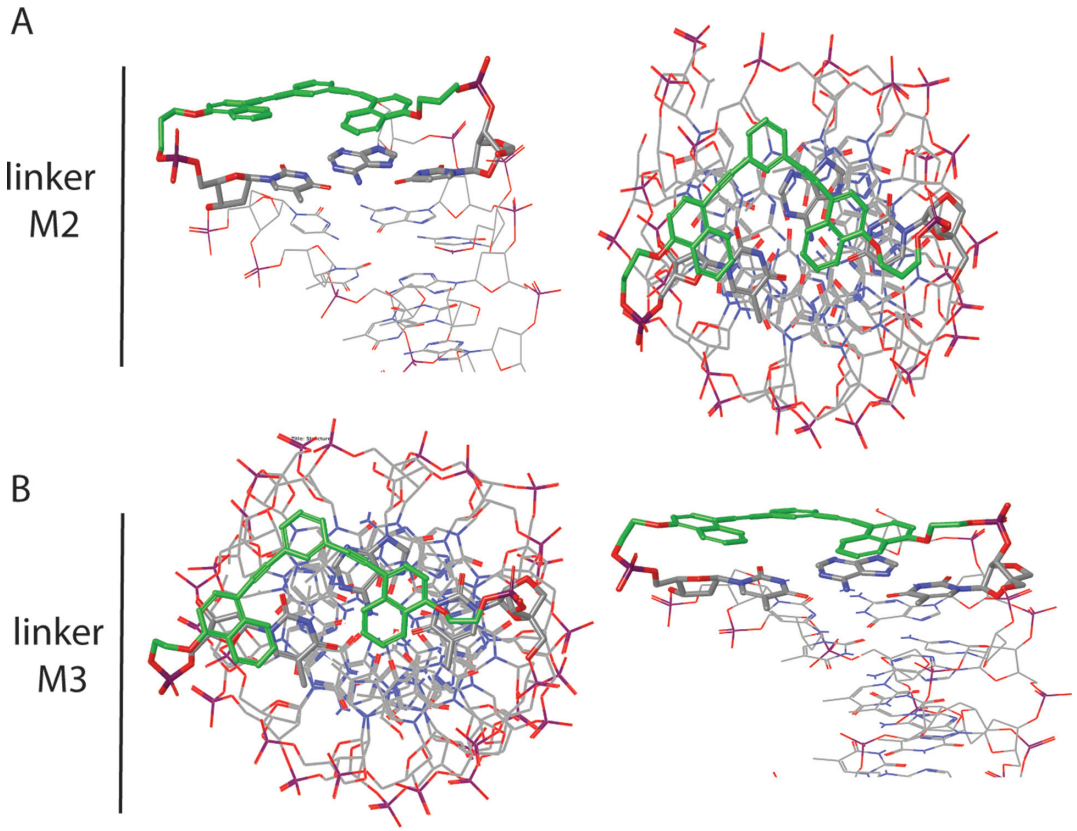

Figure 4. Modeling of the linkers M2 and M3. Top and side views from molecular modeling of a truncated triplex comprising linker M2 (upper panel) or linker M3 (lower panel) in the clamp.

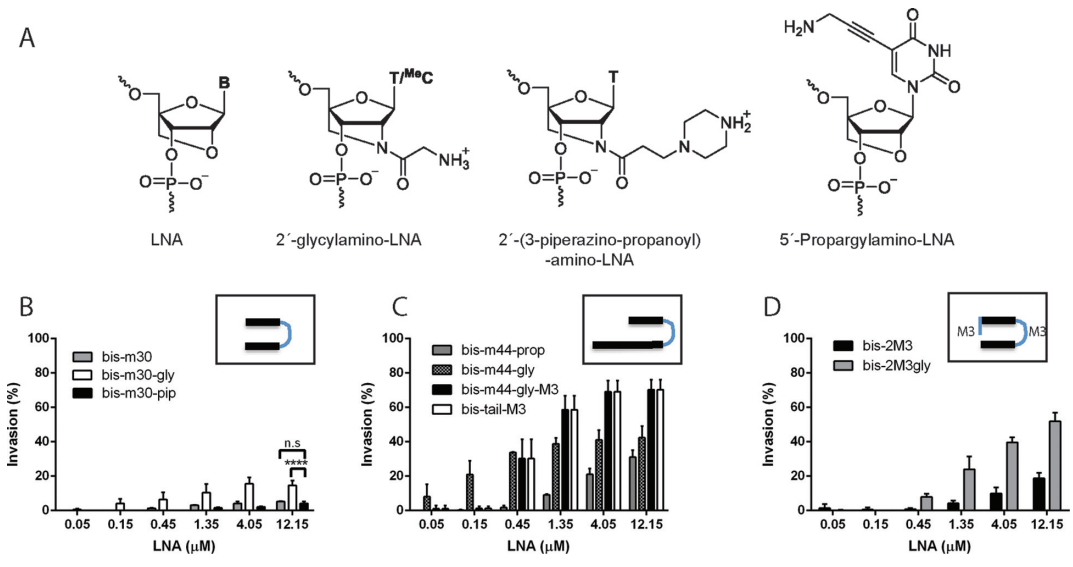

Figure 5. Functionalized LNA in bisLNAs. (**A**) Chemical structure of LNA, 5′-propargylamino-LNA, 2′-glycylamino-LNA and 2′-(3-piperazinopropanoyl)-amino-LNA. Quantification of invasion using S1 nuclease assay with (**B**) bisLNAs clamp containing unmodified LNA, 2′-glycylamino-LNA and 2′-(3-piperazinopropanoyl)-amino-LNA, (**C**) bisLNAs tail-clamp containing LNA-rich tail, linker M3, 2′-glycylamino-LNA or 5′-propargylamino-LNA (**D**) bisLNAs clamp with two M3 linkers. For (B-D), plasmid p-Del1 and bisLNAs were incubated for 16 h at 37°C at intranuclear pH and salt conditions.

duplex boundary for a M3 residue at the termini of the TFO (data not shown).

M3-containing bisLNAs require stable TFO binding to invade efficiently

We were concerned that the benefit of the linker M3, due to its stacking ability depends on the surrounding nucleobases. To investigate this, we examined bisLNAs targeting various sites from the genome (Table 2). In addition to different sequences flanking the linker M3, these bisLNAs differ in the base compositions in the TFO-arm. The bisLNA designed for the c-MYC promoter P1 contained a majority of thymines whereas the bisLNA for an estrogen response element (bis-ERE) has a mixed content of cytosine and thymine (40). The two other bisLNAs targeting respectively the c-MYC promoter P2 and the hTFF sites (41) contained a majority of cytosines, including runs of consecutive cytosines.

The DSI efficiency of M3-containing bisLNAs depends on the base composition of the TFO-arm (Figure 6). Not surprisingly, the bis-m44-M3 showed the greatest DSI (83%) under physiological conditions, while the bis-ERE with a mixed sequence was able to invade to 55% at 12 μM. In contrast, bis-m37-M3 and bis-hTFF were almost unable to invade the plasmids (21% and 13% DSI, respectively, at 12 μM). This is presumably due to the presence of runs of consecutive Cs that destabilize TFOs under physiological conditions, as a result of the pH dependence of the C^+•GC triplets. To produce more stable triplexes, these experiments were then performed at pH 5.8 under similar salt conditions. At pH 5.8, the M3-containing bisLNAs were all highly efficient with DSI > 70%, independently of their base compositions (Figure 6A–D). As expected, the C-rich ONs, bis-hTFF (79% DSI at 12 μM) and bis-m37-M3 (68% at 12 μM), exhibited the greatest improvement upon pH change. Furthermore, the M3-containing bisLNAs for c-MYC P1 and P2 (76% and 71% at 12 μM) were superior to the respective bisLNAs with 5-nt linker at acidic pH (27% and 42% at 12 μM). This suggests that the linker M3 promotes DSI also at acidic pH and stacks independently of the surrounding base composition. However, the beneficial effect of the linker M3 requires stable TFO-binding.

M3-containing bisLNAs invade specifically into their designated target

To confirm that the M3-containing bisLNAs invade at the expected site, we developed an S1 nuclease footprinting assay based on capillary electrophoresis, as opposed to gel electrophoresis (Figure 7A). Using this method, we mapped the single stranded regions, resulting from the bisLNA invasion, by using S1 nuclease probing in the plasmid pEGFP-BSf containing the MYC binding site. To amplify the fragments after S1 nuclease, we generated via primer extension a range of 6-FAM labeled DNA stretches detectable by capillary electrophoresis. The fragments were then aligned to the dideoxynucleotide-based reaction-ladders to accurately identify the terminal base of the fragments. As a result, we observed efficient S1 nuclease cleavage at a distance between 69 and 106 bases from the primer site, which suggests DSI for bis-m44-M3 at the expected polypurine site. A similar digestion pattern was observed for bis-m44 and WC-m44-M3. However, in absence of bisLNA, no significant S1 nuclease cleavage in the plasmid pEGFP-BSf was observed.

To further test the specificity, we incubated bis-m44-M3 or WC-m44-M3 with mutant plasmids that contain single or double mutations. These mutations were introduced to disrupt bisLNA binding in the clamp or tail region (Supplementary Figure S6A). Remarkably, bis-m44-M3 showed high discrimination against mutations in the triplex region (Supplementary Figure S6C). In addition, bis-m44 exhibited higher discrimination against the mutations in the tail than bis-m44-M3 (Supplementary Figure S6B). More specifically, the mutations at the tail extremity did not affect DSI of bis-m44 whereas mutations when placed at the junction duplex-triplex completely prevents invasion, which was not observed with bis-m44-M3. Notably, bis-m44-M3 showed higher specificity than WC-m44-M3 as evaluated relatively to the specific invasion of the non-mutated plasmids. As anticipated, less stable triplexes formed with mismatched dsDNA targets led to significantly lower DSI.

Rolling circle amplification (RCA)

To investigate DSI in a more complex environment, we transformed *E. coli* bacteria with plasmid pUC19-2BS containing two consecutive invasion sites for the bisLNAs. In pUC19–2BS, the intervening sequence together with parts of the bisLNA target sites creates a unique sequence available for detection via RCA (Supplementary Figure S7). This method is initiated with a local DNA unwinding with bisLNAs, followed by binding and circularization of a padlock probe via ligation. Then, the assembled padlock probe serves as a template for primer extension, which generates repetitive long DNA fragments called RCPs. Finally, the RCPs are detected via hybridization with short fluorescently labeled ONs (Figure 7B). Using this method, we detected a higher number of RCPs after incubation with bis-m44 in pUC19-2BS-transformed bacteria as compared to pUC19-transformed bacteria. In absence of bis-m44, pUC19-2BS-transformed bacteria showed limited number of RCPs, presumably arising from DNA breathing that allows padlock binding without bisLNA. Furthermore, no RCPs were detected in pUC19-transformed bacteria in absence of bisLNA. This demonstrates that bisLNA-induced DSI takes place in the full complexity of the interior of bacterial cells under physiological salt and pH conditions.

DISCUSSION

In this report, we investigated the invasion mechanism for the bisLNAs. Our findings suggest that bisLNAs bind initially via the TFO-arm followed by WC-arm hybridization (Figure 7C). Interestingly, during this Hoogsteen-first mechanism, bisLNAs form via its TFO-arm an intermediate complex that makes the underlying duplex less accessible for WC-arm invasion. This proposed mechanism reveals that regular bisLNAs, due to this effect, are not fully optimized in term of DSI and thereby allows the development of further improvements such as a novel stacking linker and 2′-glycylamino-LNAs. As a result, these modifications effi-

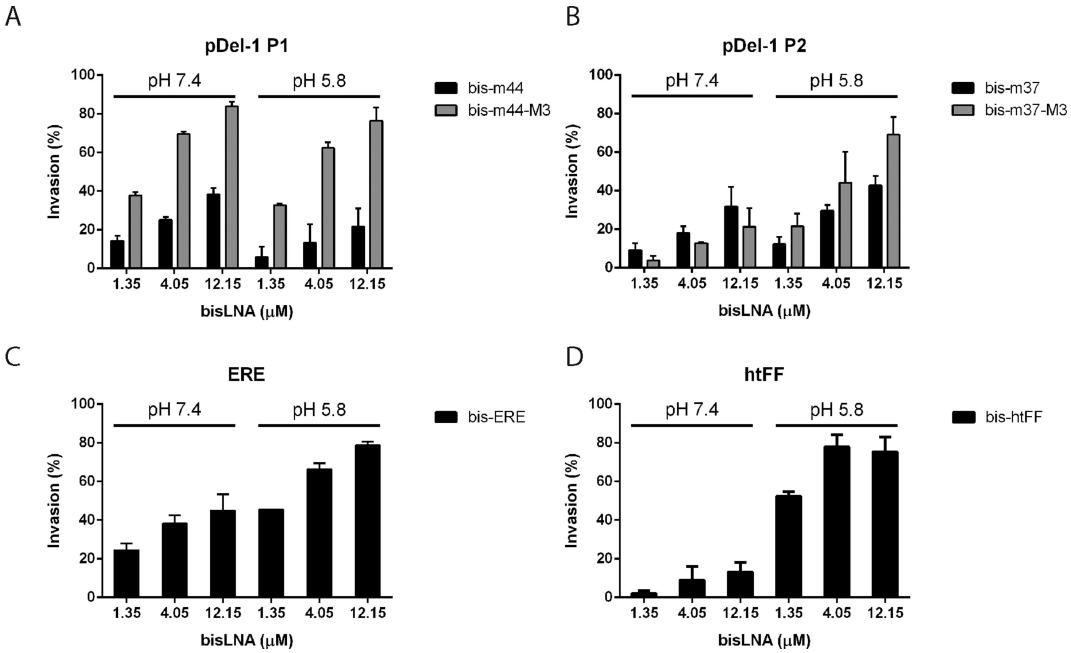

Figure 6. bisLNAs targeting various binding sites at pH 5.8 and pH 7.4. (**A**) Comparison using S1 nuclease assay between bis-m44 (left panel), bis-m37 (right panel) and the respective M3-containing bis-m44-M3 and bis-m37-M3. (**B**) Quantification of invasion using S1 nuclease assay for the bisLNAs targeting ERE site (right panel) and hTFF sites (left panel). Plasmids pDel1, p-ERE, p-hTFF and bisLNAs were incubated for 16 h at 37°C at pH 5.8 or 7.4 and intranuclear salt concentration.

ciently promote DSI compared to the unmodified bisLNAs and the corresponding non-clamp LNA-ONs.

In their initial design, bisLNAs combine HG binding to facilitate the recognition of their targets and WC binding to enhance the overall stability. However, their binding mechanism is poorly understood. As previously reported, DNA is a very fluctuant biopolymer with transient base pair openings (42,43), sufficiently dynamic to favor strand invasion of synthetic ONs. This requires typically high ON concentration (44–47) but due to the Hoogsteen-first binding, we expect bisLNAs to have superior ability to find their target along the plasmid, which enables binding at lower concentration. Our finding is that the triplex formation seems to play a balanced role between favoring and hampering DSI.

The crucial role of the TFO-arm suggests a Hoogsteen-first binding followed by a strand displacement of the WC-arm. Supporting this hypothesis, the bisLNAs forming stable triplexes (T-rich or C,T) invade efficiently. We assume that this TFO binding helps to reach the target and forms a transient complex at the invasion site to facilitate DSI. In agreement, introducing glyLNAs improves DSI by increasing TFO kinetics and stability. This is presumably due to a favorable conformational restriction that glyLNAs exhibit a better ability to interact with the negatively charged backbone, as compared to other positively charged analogues (31,48).

In contrast, the bisLNAs generating unstable triplexes (C-rich or less LNA in the TFO-arm) failed to invade efficiently. Our interpretation is that the fast dissociation of the TFO-arm hampers the bisLNA to stay in vicinity of its target to perform strand-displacement. It is known that the design of a third strand that binds to the dsDNA under physiological conditions is challenging with respect to the base composition (49). C-rich parallel TFOs are less stable at physiological pH because the cytosines require protonation for stable triplex formation (50). In particular, runs of contiguous C^+•GC triplets are even more destabilizing, since they compete for protonation and further decrease the pKa value of cytosine (51). Moreover, as reported, LNA-TFOs have similar association rate but lower dissociation rate than their oligodeoxyribonucleotide counterparts (50,52,53).

Due to its structure, the binding of a third strand to the dsDNA major groove hampers invasion into the underlying duplex. Therefore, the unlinked arms become less efficient than their corresponding WC-arm alone. This is in agreement with a recent modeling study demonstrating that the TFO binding hinders flipping of the base located on the purine strand, rendering the underlying duplex less accessible for DSI (54). As a consequence, the strand displacement is initiated in the more accessible neighboring duplex and then progress into the triplex to achieve full-length invasion.

Several experimental results support that bisLNAs initiate strand displacement after HG binding via the tail. First, as a general rule, bisLNAs with an extended tail (14 nt) are considerably more potent than the bisLNAs lacking a tail (Figure 5). Thus, reducing the length or LNA content in the tail decreased DSI in bisLNAs (25) (Figure 5C/Supplementary Figure S5B). Finally, plasmid mutations in the clamp-proximal region abolished the invasion for bis-m44 (Supplementary Figure S6B). More specifically, this suggests that DSI starts in vicinity to the duplex/triplex junction. This is consistent with structural studies showing that duplex/triplex junctions unwind DNA over the adjacent duplex as transition intermediates between A- and B-DNA forms (54,55).

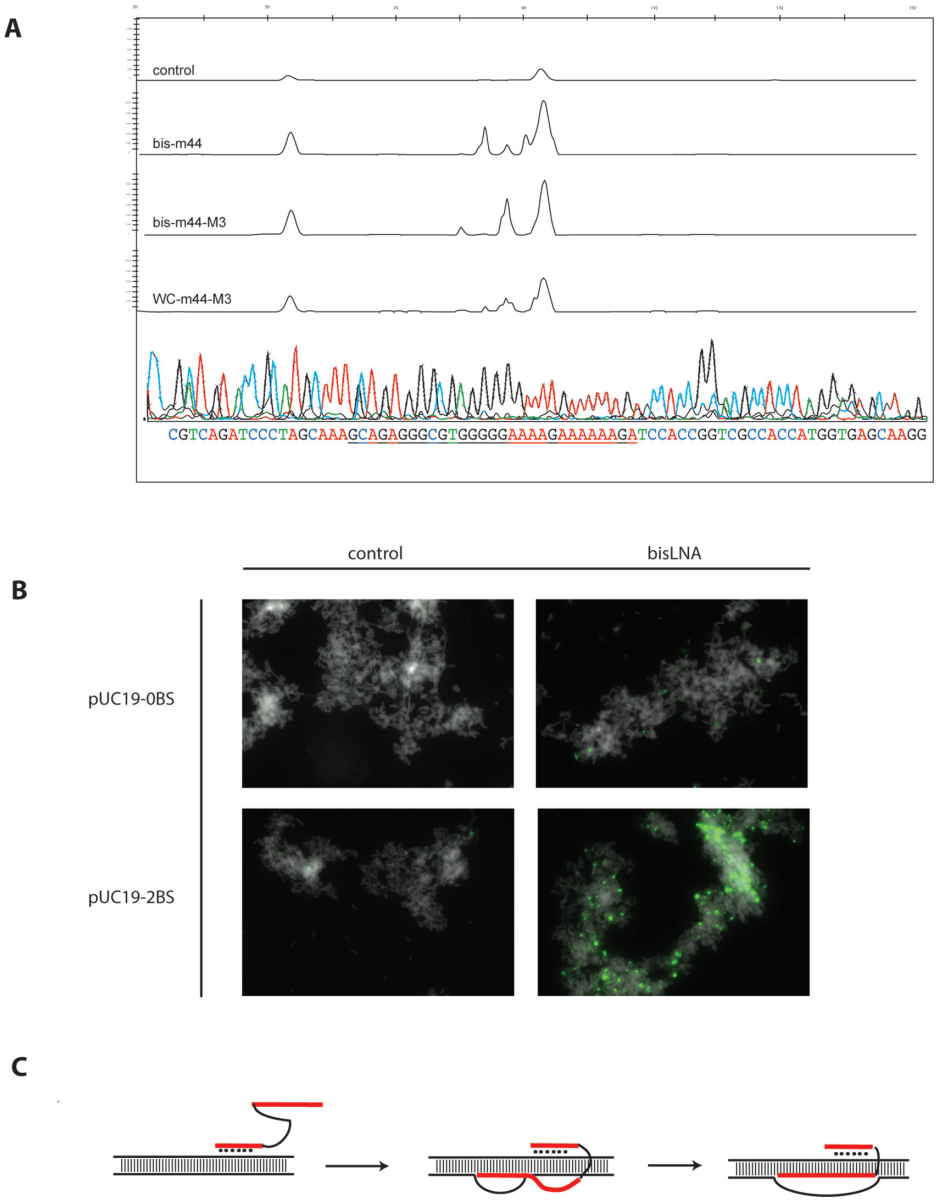

Figure 7. Sequence-specificity of bisLNA invasion into plasmids. (**A**) S1-nuclease footprinting of plasmid pEGFP-BSf hybridized with bis-m44, bis-m44-M3 and WC-m44-M3. Plasmid pEGFP-BSf was incubated 72 h at 37°C with 4 μM of the corresponding bisLNA or LNA-ON at intranuclear pH and salt conditions. In the lower panel, a sequencing ladder was superimposed with the obtained DNA fragment to identify the different S1 cleavage sites. Target sequence for bisLNA invasion site is underlined. (**B**) *In situ* detection of plasmid DNA pre-opened by bisLNA using padlock probes and rolling circle amplification (RCA). After incubation with bisLNA, *E. coli* bacteria were incubated with padlock probe for ligation and subsequently with primer for RCA. *E. coli* bacteria were then stained in blue using DAPI and rolling circle products (RCPs), shown in green, were detected using fluorescently labeled oligonucleotides. (**C**) Proposed model for bisLNA invasion into dsDNA. The bisLNA binds via TFO-arm, followed by strand displacement initiated in the tail region in the DNA duplex. Strand displacement progresses in the triplex region to achieve stable full-length invasion.

To our knowledge, stacking linkers were never specifically designed in clamp-ONs for DNA invasion. Interestingly, we found that the new linker M3 is superior to the previously described rigid linkers N2, M2 (27,28) and other flexible linkers tested (25). One major finding is that the linker structure is really crucial to provide increased π–π interaction, rigidity and thereby optimal DSI. Previously, the comparison of linker types, sequences and lengths for clamp-ONs has established that these factors can greatly affect the binding affinity to a DNA target (56). As mentioned by Kool, the linker preorganization is an important factor for DNA recognition because the linker turns a trimolecular reaction into a bimolecular one and promotes a cooperative binding of the WC- and TFO-arms (57). Moreover, by enhancing the stability of the final complex, the linker M3 favors strand displacement but also requires a tail to initiate the invasion. As an exception, the bisLNAs flanked by two M3 moieties invade efficiently without a tail. This indicates that stacking interactions at triplex-duplex junctions promote DSI despite the binding of a third strand. Due to the presence of open bases, triplex-duplex junctions are strong binding sites for intercalating molecules (55). It is noteworthy

that this strategy allows the design of shorter bisLNAs, presumably more specific than regular bisLNAs. Furthermore, bisLNA/DNA complexes with stacking moieties flanking an intervening sequence are similar to bis-intercalators, a class of DNA binders that showed very high affinity and applications in cancer therapy (58).

As reported, short linear PNAs and bisPNAs clamp invade efficiently into relaxed and supercoiled DNA under 'low salt' conditions (59). Thus, it is relevant to compare the mode of binding of bisLNAs to other clamp-ONs such as bisPNAs. However, it should be kept in mind that there are important differences between the structure, length and charge of bisPNAs and bisLNAs, obviating a direct side-by-side comparison. Rather they should be considered complementing technologies with unique characteristics. The bisPNAs bind via Hoogsteen-first mechanism but do not exhibit a similar TFO-dependent negative effect on the invasion (60). In addition, the bisPNAs clamp bind with faster kinetics than the extended bisPNAs tail-clamp (61). Surprisingly, only a few different linkers (8-amino-2,6-dioxaoctanoic or acid aminohexanoic) have been tested in bisPNAs or in other clamp ONs (57). The linker in bisPNAs is ascribed to form several isomers of triplex invasion complexes (62) but no improvement due to the linker was ever demonstrated (62,63). Therefore, our study emphasizes the role of the linker and stacking interactions for efficient DNA recognition. More importantly, it also suggests that bisLNAs have a specific mechanism of binding that differs from bisPNAs. In addition, we envisage the use of bisLNAs under physiological conditions ('high salt'), which are non-optimal for bisPNAs.

Footprinting is a well-established method (64,65) that can be used to visualize invasion, when based on S1 nuclease cleavage of opened DNA regions. Previous studies have reported the development of fluorescence-based DNaseI footprinting (66), but S1 nuclease footprinting has been traditionally performed with radioactive labeling (67). Our fluorescent-labeled approach has many advantages over traditional S1 nuclease footprinting techniques. First, this new method eliminates the need for radioactivity and polyacrylamide gel electrophoresis. Second, fluorescent dyes are more stable than ^{32}P. Therefore, fluorescently labeled fragments do not need to be prepared immediately prior to running a footprinting assay and do not require specific protection or storage. Finally, the method is faster than footprinting using polyacrylamide gel electrophoresis and can easily be automatized for large numbers of samples. The validity of the method was achieved by comparing the results obtained for bis-m44 with those previously published using radioactivity (25). Overall, this method renders S1 nuclease footprinting faster and more accessible and is complementing the S1 nuclease cleavage assay.

The rolling circle amplification enables the detection of invasion inside bacteria. Although bacterial DNA targeting strategies using bisPNAs (at 42°C in low salt buffer) were previously described by Smolina *et al.* (19,68), our method shows bisLNA binding inside bacteria under physiologically relevant conditions. Therefore, in a cellular environment, we expect the bisLNAs to bind via a Hoogsteen-first mechanism and reach their genomic DNA targets at low concentrations. Currently, the potential target sites for bisLNAs require a polypurine stretch to allow stable triplex binding. Although polypurine stretches are frequent in the genome (69), new triplex forming nucleobases may increase the range of possible target sites for the bisLNAs (70,71).

In summary, we successfully designed bisLNAs significantly more efficient than previous bisLNAs and non-clamp LNA-ONs at nanomolar concentrations. In addition, DSI was achieved inside bacteria containing the target plasmids and detected via RCA. This study shows that double-helix invasion remains a challenge, requiring new chemistry and structural insights due to the complexity of the process. However, after optimization, DNA invasion has been realized at lower concentrations than previously shown. Difficult to access DNA regions could therefore become available for targeting, which has important implications for the development of new therapeutics as well as for various aspects of bio- and nanotechnology.

SUPPLEMENTARY DATA

Supplementary Data are available at NAR Online.

ACKNOWLEDGEMENT

We thank Dr Karin Dahlman Wright and Dr Chunyan Zhao, Karolinska Institutet, for valuable discussions regarding the ERE and hTFF target sites, and Dr Pawan Kumar, University of Idaho, for providing access to intermediates needed for the synthesis of C5-propargylamino modified LNA-U phosphoramidites.

FUNDING

Swedish Medical Research Council and the Swedish Cancer Society; Y. Vladimir Pabon is indebted to the Departamento Administrativo de Ciencia, Tecnología e Innovación COLCIENCIAS [02007/24122010]; a postdoc grant from the Brain Foundation at Stockholm (to E.Z.). Funding for open access charge: The Swedish Medical Research Council.

Conflict of interest statement. None declared.

REFERENCES

1. Seeman,N.C. (2010) Nanomaterials based on DNA. *Annu. Rev. Biochem.*, **79**, 65–87.
2. Rusling,D.A. and Fox,K.R. (2014) Sequence-specific recognition of DNA nanostructures. *Methods*, **67**, 123–133.
3. Ghosh,I., Stains,C.I., Ooi,A.T. and Segal,D.J. (2006) Direct detection of double-stranded DNA: molecular methods and applications for DNA diagnostics. *Mol. BioSyst.*, **2**, 551–560.
4. Puyo,S., Montaudon,D. and Pourquier,P. (2014) From old alkylating agents to new minor groove binders. *Crit. Rev. Oncol. Hematol.*, **89**, 43–61.
5. Duca,M., Vekhoff,P., Oussedik,K., Halby,L. and Arimondo,P.B. (2008) The triple helix: 50 years later, the outcome. *Nucleic Acids Res.*, **36**, 5123–5138.
6. Hsu,P.D., Lander,E.S. and Zhang,F. (2014) Development and applications of CRISPR-Cas9 for genome engineering. *Cell*, **157**, 1262–1278.
7. Wang,T., Wei,J.J., Sabatini,D.M. and Lander,E.S. (2014) Genetic screens in human cells using the CRISPR-Cas9 system. *Science*, **343**, 80–84.

8. Sau,S.P., Madsen,A.S., Podbevsek,P., Andersen,N.K., Kumar,T.S., Andersen,S., Rathje,R.L., Anderson,B.A., Guenther,D.C., Karmakar,S. *et al.* (2013) Identification and characterization of second-generation invader locked nucleic acids (LNAs) for mixed-sequence recognition of double-stranded DNA. *J. Org. Chem.*, **78**, 9560–9570.
9. Didion,B.A., Karmakar,S., Guenther,D.C., Sau,S.P., Verstegen,J.P. and Hrdlicka,P.J. (2013) Invaders: recognition of double-stranded DNA by using duplexes modified with interstrand zippers of 2′-O-(Pyren-1-yl)methyl-ribonucleotides. *Chembiochem*, **14**, 1534–1538.
10. Yakovchuk,P., Protozanova,E. and Frank-Kamenetskii,M.D. (2006) Base-stacking and base-pairing contributions into thermal stability of the DNA double helix. *Nucleic Acids Res.*, **34**, 564–574.
11. Lenglet,G. and David-Cordonnier,M.H. (2010) DNA-destabilizing agents as an alternative approach for targeting DNA: mechanisms of action and cellular consequences. *J. Nucleic Acids*, **2010**, 290935.
12. Kool,E.T. (2001) Hydrogen bonding, base stacking, and steric effects in dna replication. *Annu. Rev. Biophys. Biomol. Structure*, **30**, 1–22.
13. Nielsen,P.E., Egholm,M., Berg,R.H. and Buchardt,O. (1991) Sequence-selective recognition of DNA by strand displacement with a thymine-substituted polyamide. *Science*, **254**, 1497–1500.
14. He,G., Rapireddy,S., Bahal,R., Sahu,B. and Ly,D.H. (2009) Strand invasion of extended, mixed-sequence B-DNA by gammaPNAs. *J. Am. Chem. Soc.*, **131**, 12088–12090.
15. Rapireddy,S., Bahal,R. and Ly,D.H. (2011) Strand invasion of mixed-sequence, double-helical B-DNA by gamma-peptide nucleic acids containing G-clamp nucleobases under physiological conditions. *Biochemistry*, **50**, 3913–3918.
16. Janowski,B.A., Kaihatsu,K., Huffman,K.E., Schwartz,J.C., Ram,R., Hardy,D., Mendelson,C.R. and Corey,D.R. (2005) Inhibiting transcription of chromosomal DNA with antigene peptide nucleic acids. *Nat. Chem. Biol.*, **1**, 210–215.
17. Egholm,M., Christensen,L., Dueholm,K.L., Buchardt,O., Coull,J. and Nielsen,P.E. (1995) Efficient pH-independent sequence-specific DNA binding by pseudoisocytosine-containing bis-PNA. *Nucleic Acids Res.*, **23**, 217–222.
18. Ray,A. and Norden,B. (2000) Peptide nucleic acid (PNA): its medical and biotechnical applications and promise for the future. *FASEB J.*, **14**, 1041–1060.
19. Smolina,I.V. and Frank-Kamenetskii,M.D. (2014) PNA openers and their applications for bacterial DNA diagnostics. *Methods Mol. Biol.*, **1050**, 121–130.
20. Zaghloul,E.M., Madsen,A.S., Moreno,P.M., Oprea,II, El-Andaloussi,S., Bestas,B., Gupta,P., Pedersen,E.B., Lundin,K.E., Wengel,J. *et al.* (2011) Optimizing anti-gene oligonucleotide 'Zorro-LNA' for improved strand invasion into duplex DNA. *Nucleic Acids Res.*, **39**, 1142–1154.
21. Ge,R., Heinonen,J.E., Svahn,M.G., Mohamed,A.J., Lundin,K.E. and Smith,C.I. (2007) Zorro locked nucleic acid induces sequence-specific gene silencing. *FASEB J.*, **21**, 1902–1914.
22. Hertoghs,K.M., Ellis,J.H. and Catchpole,I.R. (2003) Use of locked nucleic acid oligonucleotides to add functionality to plasmid DNA. *Nucleic Acids Res.*, **31**, 5817–5830.
23. Vester,B. and Wengel,J. (2004) LNA (locked nucleic acid): high-affinity targeting of complementary RNA and DNA. *Biochemistry*, **43**, 13233–13241.
24. Lundin,K.E., Hojland,T., Hansen,B.R., Persson,R., Bramsen,J.B., Kjems,J., Koch,T., Wengel,J. and Smith,C.I. (2013) Biological activity and biotechnological aspects of locked nucleic acids. *Adv. Genet.*, **82**, 47–107.
25. Moreno,P.M., Geny,S., Pabon,Y.V., Bergquist,H., Zaghloul,E.M., Rocha,C.S., Oprea,II, Bestas,B., Andaloussi,S.E., Jorgensen,P.T. *et al.* (2013) Development of bis-locked nucleic acid (bisLNA) oligonucleotides for efficient invasion of supercoiled duplex DNA. *Nucleic Acids Res.*, **41**, 3257–3273.
26. Bomholt,N., Osman,A.M. and Pedersen,E.B. (2008) High physiological thermal triplex stability optimization of twisted intercalating nucleic acids (TINA). *Org. Biomol. Chem.*, **6**, 3714–3722.
27. Filichev,V.V., Nielsen,M.C., Bomholt,N., Jessen,C.H. and Pedersen,E.B. (2006) High thermal stability of 5′-5′-linked alternate hoogsteen triplexes at physiological pH. *Angew. Chem. Int. Ed. Engl.*, **45**, 5311–5315.
28. Fatthalla,M.I. and Pedersen,E.B. (2012) Improved DNA clamps by stacking to adjacent nucleobases. *Helv. Chim. Acta*, **95**, 1538–1547.
29. Astakhova,I.K. and Wengel,J. (2014) Scaffolding along nucleic acid duplexes using 2′-amino-locked nucleic acids. *Acc. Chem. Res.*, **47**, 1768–1777.
30. Johannsen,M.W., Crispino,L., Wamberg,M.C., Kalra,N. and Wengel,J. (2011) Amino acids attached to 2′-amino-LNA: synthesis and excellent duplex stability. *Org. Biomol. Chem.*, **9**, 243–252.
31. Hojland,T., Kumar,S., Babu,B.R., Umemoto,T., Albaek,N., Sharma,P.K., Nielsen,P. and Wengel,J. (2007) LNA (locked nucleic acid) and analogs as triplex-forming oligonucleotides. *Org. Biomol. Chem.*, **5**, 2375–2379.
32. Kumar,P., Ostergaard,M.E., Baral,B., Anderson,B.A., Guenther,D.C., Kaura,M., Raible,D.J., Sharma,P.K. and Hrdlicka,P.J. (2014) Synthesis and biophysical properties of C5-functionalized LNA (locked nucleic acid). *J. Org. Chem.*, **79**, 5047–5061.
33. Filichev,V.V. and Pedersen,E.B. (2005) Stable and selective formation of hoogsteen-type triplexes and duplexes using twisted intercalating nucleic acids (TINA) prepared via postsynthetic Sonogashira solid-phase coupling reactions. *J. Am. Chem. Soc.*, **127**, 14849–14858.
34. Hellman,L.M. and Fried,M.G. (2007) Electrophoretic mobility shift assay (EMSA) for detecting protein-nucleic acid interactions. *Nat. Protoc.*, **2**, 1849–1861.
35. Lundin,K.E., Hasan,M., Moreno,P.M., Tornquist,E., Oprea,I., Svahn,M.G., Simonson,E.O. and Smith,C.I. (2005) Increased stability and specificity through combined hybridization of peptide nucleic acid (PNA) and locked nucleic acid (LNA) to supercoiled plasmids for PNA-anchored 'Bioplex' formation. *Biomol. Eng.*, **22**, 185–192.
36. Yoon,K., Hobbs,C.A., Walter,A.E. and Turner,D.H. (1993) Effect of a 5′-phosphate on the stability of triple helix. *Nucleic Acids Res.*, **21**, 601–606.
37. Lou,C., Vester,B. and Wengel,J. (2015) Oligonucleotides containing a piperazino-modified 2′-amino-LNA monomer exhibit very high duplex stability and remarkable nuclease resistance. *Chem. Commun.*, **51**, 4024–4027.
38. Skov,J., Bryld,T., Lindegaard,D., Nielsen,K.E., Hojland,T., Wengel,J. and Petersen,M. (2011) Synthesis and structural characterization of piperazino-modified DNA that favours hybridization towards DNA over RNA. *Nucleic Acids Res.*, **39**, 1953–1965.
39. Sau,S.P., Kumar,P., Anderson,B.A., Ostergaard,M.E., Deobald,L., Paszczynski,A., Sharma,P.K. and Hrdlicka,P.J. (2009) Optimized DNA-targeting using triplex forming C5-alkynyl functionalized LNA. *Chem. Commun.*, 6756–6758.
40. Klinge,C.M. (2001) Estrogen receptor interaction with estrogen response elements. *Nucleic Acids Res.*, **29**, 2905–2919.
41. Berry,M., Nunez,A.M. and Chambon,P. (1989) Estrogen-responsive element of the human pS2 gene is an imperfectly palindromic sequence. *Proc. Natl. Acad. Sci. U.S.A.*, **86**, 1218–1222.
42. von Hippel,P.H., Johnson,N.P. and Marcus,A.H. (2013) Fifty years of DNA 'Breathing': reflections on old and new approaches. *Biopolymers*, **99**, 923–954.
43. Timsit,Y. (2012) DNA-directed base pair opening. *Molecules*, **17**, 11947–11964.
44. Lohse,J., Dahl,O. and Nielsen,P.E. (1999) Double duplex invasion by peptide nucleic acid: a general principle for sequence-specific targeting of double-stranded DNA. *Proc. Natl. Acad. Sci. U.S.A*, **96**, 11804–11808.
45. Bentin,T. and Nielsen,P.E. (1996) Enhanced peptide nucleic acid binding to supercoiled DNA: possible implications for DNA 'breathing' dynamics. *Biochemistry*, **35**, 8863–8869.
46. Demidov,V.V., Yavnilovich,M.V. and Frank-Kamenetskii,M.D. (1997) Kinetic analysis of specificity of duplex DNA targeting by homopyrimidine peptide nucleic acids. *Biophys. J.*, **72**, 2763–2769.
47. Braasch,D.A. and Corey,D.R. (2001) Locked nucleic acid (LNA): fine-tuning the recognition of DNA and RNA. *Chem. Biol.*, **8**, 1–7.
48. Madsen,A.S., Jorgensen,A.S., Jensen,T.B. and Wengel,J. (2012) Large scale synthesis of 2′-amino-LNA thymine and 5-methylcytosine nucleosides. *J. Org. Chem.*, **77**, 10718–10728.
49. Cheng,Y.K. and Pettitt,B.M. (1992) Stabilities of double- and triple-strand helical nucleic acids. *Prog. Biophys. Mol. Biol.*, **58**, 225–257.
50. Sun,B.W., Babu,B.R., Sorensen,M.D., Zakrzewska,K., Wengel,J. and Sun,J.S. (2004) Sequence and pH effects of LNA-containing triple

helix-forming oligonucleotides: physical chemistry, biochemistry, and modeling studies. *Biochemistry*, **43**, 4160–4169.
51. James,P.L., Brown,T. and Fox,K.R. (2003) Thermodynamic and kinetic stability of intermolecular triple helices containing different proportions of C+*GC and T*AT triplets. *Nucleic Acids Res.*, **31**, 5598–5606.
52. Koizumi,M., Morita,K., Daigo,M., Tsutsumi,S., Abe,K., Obika,S. and Imanishi,T. (2003) Triplex formation with 2′-O,4′-C-ethylene-bridged nucleic acids (ENA) having C3'-endo conformation at physiological pH. *Nucleic Acids Res.*, **31**, 3267–3273.
53. Sau,S.P., Kumar,P., Sharma,P.K. and Hrdlicka,P.J. (2012) Fluorescent intercalator displacement replacement (FIDR) assay: determination of relative thermodynamic and kinetic parameters in triplex formation–a case study using triplex-forming LNAs. *Nucleic Acids Res.*, **40**, e162.
54. Esguerra,M., Nilsson,L. and Villa,A. (2014) Triple helical DNA in a duplex context and base pair opening. *Nucleic Acids Res.*, **42**, 11329–11338.
55. Collier,D.A., Mergny,J.L., Thuong,N.T. and Helene,C. (1991) Site-specific intercalation at the triplex-duplex junction induces a conformational change which is detectable by hypersensitivity to diethylpyrocarbonate. *Nucleic Acids Res.*, **19**, 4219–4224.
56. Rumney,S. and Kool,E.T. (1995) Structural optimization of non-nucleotide loop replacements for duplex and triplex DNAs. *J. Am. Chem. Soc.*, **117**, 5635–5646.
57. Kool,E.T. (1997) Preorganization of DNA: design principles for improving nucleic acid recognition by synthetic oligonucleotides. *Chem. Rev.*, **97**, 1473–1488.
58. Zolova,O.E., Mady,A.S. and Garneau-Tsodikova,S. (2010) Recent developments in bisintercalator natural products. *Biopolymers*, **93**, 777–790.
59. Nielsen,P.E. (2010) Sequence-selective targeting of duplex DNA by peptide nucleic acids. *Curr. Opin. Mol. Ther.*, **12**, 184–191.
60. Hansen,M.E., Bentin,T. and Nielsen,P.E. (2009) High-affinity triplex targeting of double stranded DNA using chemically modified peptide nucleic acid oligomers. *Nucleic Acids Res.*, **37**, 4498–4507.
61. Kaihatsu,K., Shah,R.H., Zhao,X. and Corey,D.R. (2003) Extending recognition by peptide nucleic acids (PNAs): binding to duplex DNA and inhibition of transcription by tail-clamp PNA-peptide conjugates. *Biochemistry*, **42**, 13996–14003.
62. Hansen,G.I., Bentin,T., Larsen,H.J. and Nielsen,P.E. (2001) Structural isomers of bis-PNA bound to a target in duplex DNA. *J. Mol. Biol.*, **307**, 67–74.
63. Kuhn,H., Demidov,V.V., Nielsen,P.E. and Frank-Kamenetskii,M.D. (1999) An experimental study of mechanism and specificity of peptide nucleic acid (PNA) binding to duplex DNA. *J. Mol. Biol.*, **286**, 1337–1345.
64. Hampshire,A.J., Rusling,D.A., Broughton-Head,V.J. and Fox,K.R. (2007) Footprinting: a method for determining the sequence selectivity, affinity and kinetics of DNA-binding ligands. *Methods*, **42**, 128–140.
65. Galas,D.J. and Schmitz,A. (1978) DNAse footprinting: a simple method for the detection of protein-DNA binding specificity. *Nucleic Acids Res.*, **5**, 3157–3170.
66. Zianni,M., Tessanne,K., Merighi,M., Laguna,R. and Tabita,F.R. (2006) Identification of the DNA bases of a DNase I footprint by the use of dye primer sequencing on an automated capillary DNA analysis instrument. *J. Biomol. Tech.*, **17**, 103–113.
67. Demidov,V., Frank-Kamenetskii,M.D., Egholm,M., Buchardt,O. and Nielsen,P.E. (1993) Sequence selective double strand DNA cleavage by peptide nucleic acid (PNA) targeting using nuclease S1. *Nucleic Acids Res.*, **21**, 2103–2107.
68. Smolina,I., Lee,C. and Frank-Kamenetskii,M. (2007) Detection of low-copy-number genomic DNA sequences in individual bacterial cells by using peptide nucleic acid-assisted rolling-circle amplification and fluorescence in situ hybridization. *Appl. Environ. Microbiol.*, **73**, 2324–2328.
69. Goni,J.R., de la Cruz,X. and Orozco,M. (2004) Triplex-forming oligonucleotide target sequences in the human genome. *Nucleic Acids Res.*, **32**, 354–360.
70. Malnuit,V., Duca,M. and Benhida,R. (2011) Targeting DNA base pair mismatch with artificial nucleobases. Advances and perspectives in triple helix strategy. *Org. Biomol. Chem.*, **9**, 326–336.
71. Fox,K.R. and Brown,T. (2011) Formation of stable DNA triplexes. *Biochem. Soc. Trans.*, **39**, 629–634.